Gas-Phase Bond Strength and Atomic Connectivity Studies of the Unsymmetrical Two-Center Three-Electron Ion, $[Et_2S\therefore SMe_2]^+$

Mary A. James, Michael L. McKee,* and Andreas J. Illies*

Contribution from the Department of Chemistry, Auburn University, Auburn University, Alabama 36849-5312

Received February 12, 1996[⊗]

Abstract: A computational and experimental study of the unsymmetrical 2c−3e bond in $[Et_2S\therefore SMe_2]^+$ is presented. For the first time, MS/MS collision-induced dissociation experiments provide strong experimental support of the atomic connectivity in a gas-phase S∴S 2c−3e association adduct. The strongest peak in the collision-induced dissociation spectrum corresponds to Et_2S^+, consistent with the lower ionization potential of Et_2S compared to Me_2S and the proposed structure. High-pressure equilibrium mass spectrometry experiments yield a reaction enthalpy of −104 kJ/mol for the equilibrium reaction $Et_2S^+ + Me_2S \rightleftarrows [Et_2S\therefore SMe_2]^+$ at 506 K. Correcting this value to 0 K using *ab initio* molecular parameters results in a bond energy of 107 kJ/mol which can be compared to a calculated value of 107.9 kJ/mol at the B3LYP/6-31G(d)//B3LYP/6-31G(d)+ZPC level. Studies on a competing reaction, $Et_2S^+ + Et_2S \rightleftarrows [Et_2S\therefore SEt_2]^+$, yield an experimental bond enthalpy of 119 kJ/mol at 506 K and a calculated bond energy of 121.3 kJ/mol, in excellent agreement with previously reported values.

Introduction

Two-center three-electron bonds, 2c−3e or $(\sigma)^2(\sigma^*)^1$, were first described by Pauling in 1931 and can be represented by the following molecular orbital diagram.[1]

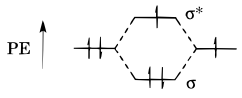

$[A\therefore A]^+$

In the years since the first description by Pauling, a great deal of interest has been expressed in such systems and a large number of molecules containing these bonds have been identified in solution.[2,3] Despite this interest, very few experiments have probed the nature of these bonds in the gas phase. Over the past few years our group has had an interest in 2c−3e sulfur−sulfur bonding in reaction intermediates and in association products of gas-phase ion−molecule reactions. We have recently published theoretical S∴S bond energies for the bonds in $[H_2S\therefore SH_2]^+$ and $[c\text{-}C_2H_4S\therefore c\text{-}SC_2H_4]^+$ and theoretical and experimental results for $[Me_2S\therefore SMe_2]^+$ and $[Et_2S\therefore SEt_2]^+$.[2,4] The bond energies for these complexes are in the range of 115 to 125 kJ/mol. In each case, the theoretical results indicate that the bond is localized between the two sulfur atoms, that both sulfur atoms have equal unpaired electron density, and that the S∴S bond length is about 30% longer than an average S−S single bond length.[5] The bond strengths (about 45% of a S−S single bond energy, ≈268 kJ/mol)[6] and spin densities are consistent with the simple molecular orbital picture which predicts a bond order of $^1/_2$.

In the present paper, we present a thorough experimental and computational study on the sulfur−sulfur interaction in the unsymmetric ion $[Et_2S\therefore SMe_2]^+$. Since the two moieties Et_2S and Me_2S have different ionization potentials (8.43 and 8.710 eV, respectively),[7,8] the interacting molecular orbitals will have different energies and the resulting bond is expected to be weaker than the symmetric sulfides studied previously. The molecular-orbital diagram below more accurately represents this situation.

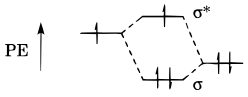

$[A\therefore X]^+$

Aqueous solution studies of such unsymmetric ions formed by pulsed radiolysis have been reported by Asmus et al.[9,10] Optical absorption spectra were observed for unsymmetric ions with 2c−3e bonding through two different heteroatoms and with 2c−3e bonding through the same heteroatoms but with different R groups. Although λ_{max} has been correlated with the 2c−3e bond strengths in these studies, this analysis has been questioned[3,11,12]

⊗ Abstract published in *Advance ACS Abstracts,* August 1, 1996.

(1) Pauling, L. *J. Am. Chem. Soc.* **1931**, *53*, 3225.

(2) For leading references see: Deng, Y.; Illies, A.; James, M. A.; McKee, M. L.; Peschke, M. *J. Am. Chem. Soc.* **1995**, *117*, 420.

(3) For leading references also see: (a) Asmus, K.-D. In *Sulfur-Centered Reaction Intermediates in Chemistry and Biology*; Chatgilialoglu, C., Asmus, K.-D., Eds.; Plenum Press: New York, 1990; p 155. (b) Hungerbuhler, H.; Guha, S. N.; Asmus, K.-D. *J. Chem. Soc., Chem. Commun.* **1991**, 999. (c) Bobrowski, K.; Schoneich, C.; Holcman, J.; Asmus, K.-D. *J. Chem. Soc., Perkin Trans. 2* **1991**, 353. (d) Mohan, H.; Asmus, K.-D. *J. Phys. Chem.* **1988**, *92*, 118.

(4) Ekern, S.; Illies, A.; McKee, M. L.; Peschke, M. *J. Am. Chem. Soc.* **1993**, *115*, 12510.

(5) (a) Knop, O.; Boyd, R. J.; Choi, S. C. *J. Am. Chem. Soc.* **1988**, *110*, 7299. (b) Allen, F. H.; Kennard, O.; Watson, D. G.; Brammer, L.; Orpen, A. G.; Taylor, R. *J. Chem. Soc., Perkin Trans. 2* **1987**, S1.

(6) Chang, R. *Chemistry*, 5th ed.; McGraw-Hill, Inc.: New York, 1994; p 360.

(7) Lias, S. G.; Bartmess, J. E.; Liebman, J. F.; Holmes, J. L.; Levin, R. D.; Mallard, W. G. Gas-Phase Ion and Neutral Thermochemistry. *J. Phys. Chem. Ref. Data* **1988**, *17*, Suppl. 1.

(8) Morgan, R. A.; Orr-Ewing, A. J.; Ashfold, M. N. R.; Wybren, J. B.; Wales, N. P. L.; de Lange, C. A. *J. Chem. Soc., Faraday Trans.* **1995**, *91*, 3339.

(9) Chaudhri, S. A.; Gobl, M.; Freyholdt, T.; Asmus, K.-D. *J. Am. Chem. Soc.* **1984**, *106*, 5988.

(10) Chaudhri, S. A.; Mohan, H.; Anklam, E.; Asmus, K.-D. *J. Chem. Soc., Perkin Trans. 2* **1996**, 383.

(11) Clark, T. *J. Comput. Chem.* **1981**, *2*, 261.

S0002-7863(96)00455-6 CCC: $12.00

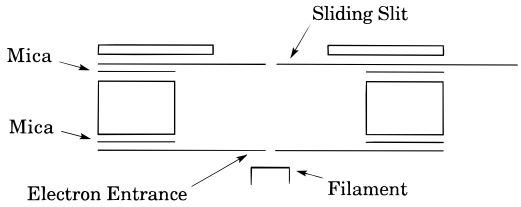

Figure 1. Variable-temperature coaxial electron entrance/ion exit ion source built for studying association reactions on the ZAB.

since the optical transition "results from a "σ-lone pair" interaction and the singly occupied σ^* energy level"[10] rather than a σ to σ^* transition.

In the present work, the experimental goals are to (1) determine $\Delta G°_{rxn}$ from equilibrium studies, (2) determine $\Delta H°_{rxn}$ and $\Delta S°_{rxn}$ from the dependence of $\Delta G°_{rxn}$ on temperature, and (3) confirm the experimental atomic connectivity from MS/MS studies for $[Et_2S\therefore SMe_2]^+$. Theoretically, the goals include calculating the bond energy, bond enthalpy, molecular entropy, ionization potentials, molecular geometries, and electron densities. This work offers the first comprehensive study of the bonding and atomic connectivity in an unsymmetric S∴S 2c−3e bonded gas-phase molecule. Unsuccessful attempts to measure the binding strength for $[Me_2S\therefore SH_2]^+$ are also briefly described.

Experimental Methods

Two mass spectrometers were used for the experimental part of this study. Ion−molecule equilibrium experiments were carried out in a highly modified DuPont 491B mass spectrometer which has recently been described in detail.[2,4] Briefly, time-resolved and continuous high-pressure ion−molecule equilibrium experiments were conducted as a function of temperature in an ion source which resembles a short drift tube. The ionizing electron entrance and ion exit apertures are arranged coaxially which allows the use of low ionizing electron energies. Great care has been taken to ensure that the ion source parts near the ion exit are all in good thermal contact with the ion source body, hence the gas temperature is uniform and well-known. The source body temperature is measured with a platinum resistance thermometer as well as a K-type thermocouple. Gas pressure in the ion source are measured with a MKS Baratron capacitance manometer.

For the present equilibrium experiments, diethyl sulfide and dimethyl sulfide (Aldrich) were distilled independently. Mixtures of diethyl sulfide and dimethyl sulfide were then prepared on a glass vacuum rack with a base pressure of about 5×10^{-6} Torr and transferred into glass bulbs with Teflon vacuum stopcocks. The gas composition was measured with a brass diaphragm gauge (±3%). Research grade N_2O (Air Products), used as a bath gas, was also stored in a glass bulb. These samples were introduced into the mass spectrometer through Granville-Phillips series 203 leak values connected to a stainless steel and glass inlet system. The reactant gas composition was 10 and 18 mol % diethyl sulfide in dimethyl sulfide while ion source compositions ranged from 1 to 8 mol % of the above mixtures in N_2O. Total ion source pressures ranged from 0.225 to 0.900 Torr and ion extraction voltages ranged from 0.50 to 10.00 V.

MS/MS experiments on the structure of $[Et_2S\therefore SMe_2]^+$ were carried out on a modified ZAB 1F. The instrument was modified by (1) installation of a variable-temperature ion source, (2) addition of a collision cell in the second field-free region, and (3) interfacing the mass-analyzed ion kinetic energy spectrometry scan (MIKES) to a PC through a Cyber Research PC-166 16 bit D/A board and signal detection through a Modern Instrumentation Technologies Inc. MTS 100 pulse preamplifier connected to a Cyber Research CYRCTM 05 timer/counter board. The scanning/data collection software was written in Microsoft Quick Basic for DOS. The new ZAB ion source, shown in Figure 1, has not yet been described in the literature. It consists of a copper block with a 0.75 cm drift length and an inside diameter of 2.54 cm. The width to length ratio is 3.4/1, thus the equipotential field lines inside the source are uniform over the entire area covered by the ion exit slits. A heat transfer tube, through which temperature-controlled air can be passed, is silver soldered to the source block. The electron entrance plate is made from 0.008 cm thick beryllium−copper plate which has a 0.025 cm hole which is insulated from the main source block by a mica gasket. The ion exit region consists of another beryllium−copper plate 0.076 cm thick with a milled channel through which a sliding EI/CI slit moves. This plate is also insulated from the source block by a mica gasket. The sliding slit itself was fabricated from 0.008 cm thick beryllium−copper; the EI slit is 0.55 cm × 0.15 cm while the CI slit is 0.55 cm × 0.010 cm. The electric potentials to the ion exit, source block, and electron entrance are controlled by the V.G. source and repeller controls with a dividing resisters network for the block potential. The advantages of this source are the following: (1) high sensitivity using low electron energies in either CI or EI modes, (2) relatively uniform electric-field gradient within the source, and (3) temperature control over the range 77−600 K. Association reactions, and hence cluster formation, are thus readily promoted at high ion-source pressures and at lower temperatures (typically 273−473 K).

The second field-free region collision cell (1 cm long, fabricated from OFHC Cu) is placed just before the second field-free region β slit. Metastable scans were carried out at the second field-free region base pressure of about 2×10^{-8} Torr using multiple scanning methods. Collision-induced dissociation (CID) experiments were also carried out with helium as a collision gas (40% main beam intensity reduction) using multiple scanning methods.

Computational Method

Calculations were performed using the GAUSSIAN94 program system.[13] Geometries were fully optimized within the appropriate point group and frequencies were calculated at the HF/6-31G(d) and B3LYP/6-31G(d) levels.[14,15] Two levels of theory used in this study will be referred to as "PMP2" and "DFT". The lower level of theory (PMP2) uses HF/6-31G(d) geometries with single-point energies at the PMP2/6-31G(d) level ("P" indicates spin-projected MP2 energies), zero-point corrections (0.9 weighting factor), and heat capacity corrections to 298 K using unscaled frequencies. The higher level of theory (DFT) uses B3LYP/6-31G(d) optimized geometries with zero-point (unscaled frequencies) and heat capacity corrections. With an appropriate choice of gradient correction and modest basis set, DFT has been shown to give results of near chemical quality.[16] In addition, spin contamination does not seem to be as serious for DFT compared to HF theory.[17] Due to resource limitations, the B3LYP/6-31G(d) frequencies were calculated for all monomers but for only two complexes, $[Me_2S\therefore SMe_2]^+$

(12) Bally, T. In *Radical Ionic Systems*; Lund, A., Shiotani, M., Eds.; Kluwer Academic Publishers: The Netherlands, 1991; pp 3−54.

(13) Frisch, M. J.; Trucks, G. W.; Schlegel, H. B.; Gill, P. M. W.; Johnson, B. G.; Robb, M. A.; Cheeseman, J. R.; Keith, T.; Petersson, G. A.; Montgomery, J. A.; Raghavachari, K.; Al-Laham, M. A.; Zakrzewski, V. G.; Ortiz, J. V.; Foresman, J. B.; Cioslowski, J.; Stefanov, B. B.; Nanayakkara, A.; Challacombe, M.; Peng, C. Y.; Ayala, P. Y.; Chen, W.; Wong, M. W.; Andres, J. L.; Replogle, E. S.; Gomperts, R.; Martin, R. L.; Fox, D. J.; Binkley, J. S.; Defrees, D. J.; Baker, J.; Stewart, J. P.; Head-Gordon, M.; Gonzalez, C.; Pople, J. A. Gaussian94 (Rev. B.1), Gaussian, Inc.: Pittsburgh, PA, 1995.

(14) For a general description of basis sets see: Hehre, W. J.; Radom, L.; Schleyer, P. v. R.; Pople, J. A. *Ab Initio Molecular Orbital Theory*; Wiley: New York, 1986.

(15) For a general description of the DFT method see: (a) Parr, R. G.; Yang, W. Density-Functional Theory of Atoms and Molecules; Oxford Press: Oxford, 1989. (b) Ziegler, T. *Chem. Rev.* **1991**, *91*, 651. (c) *Density Functional Methods in Chemistry*; Labanowski, J. K., Andzelm, J. W., Eds.; Springer: Berlin, 1991.

(16) (a) Gill, P. M. W.; Johnson, B. G.; Pople, J. A.; Frisch, M. *J. Chem. Phys. Lett.* **1992**, *197*, 499. (b) Johnson, B. G.; Gill, P. M. W.; Pople, J. A. *J. Chem. Phys.* **1993**, *98*, 5612. (c) Becke, A. D. *J. Chem. Phys.* **1993**, *98*, 5648. (d) Stevens, P. J.; Devlin, F. J.; Chablowski, C. F.; Frisch, M. J. *J. Phys. Chem.* **1994**, *98*, 11623. (e) Raghavachari, K.; Strout, D. L.; Odom, G. K.; Scuseria, G. E.; Pople, J. A.; Johnson, B. G.; Gill, P. M. W. *Chem. Phys. Lett.* **1993**, *214*, 357. (f) Raghavachari, K.; Zhang, B.; Pople, J. A.; Johnson, B. G.; Gill, P. M. W. *Chem. Phys. Lett.* **1994**, *220*, 1994. (g) Johnson, B. G.; Gonzales, C. A.; Gill, P. M. W.; Pople, J. A. *Chem. Phys. Lett.* **1994**, *221*, 100.

(17) (a) Baker, J.; Scheiner, A.; Andzelm, J. *Chem. Phys. Lett.* **1993**, *216*, 380. (b) Austen, M.; Eriksson, L. A.; Boyd, R. J. *Can. J. Chem.* **1994**, *72*, 695. (c) Eriksson, L. A.; Malkina, O. L.; Malkin, V. G.; Salahub, D. R. *J. Chem. Phys.* **1994**, *100*, 5066. (d) Qin, Y.; Wheeler, R. A. *J. Chem. Phys.* **1995**, *102*, 1689. (e) Barone, V. *Theor. Chim. Acta* **1995**, *91*, 113. (f) Adamo, C.; Barone, V.; Fortunelli, A. *J. Chem. Phys.* **1995**, *102*, 384.

and $[Et_2S\therefore SMe_2]^+$. Estimates at the DFT level for the zero-point energy, heat capacity correction, and entropy of $[Et_2S\therefore SEt_2]^+$ were made by scaling the HF/6-31G(d) value. The DFT:HF scaling factor was obtained from the $[Me_2S\therefore SMe_2]^+$ and $[Et_2S\therefore SMe_2]^+$ complexes by calculating the B3LYP/6-31G(d):HF/6-31G(d) ratio for the zero-point energy (0.935), heat capacity corrections (1.058), and entropy (1.038).

Results and Discussion

High-Pressure Mass Spectra. A typical reconstructed experimental mass spectrum measured using low ionizing electron energy (10 eV) for a 5% Et_2S in Me_2S mixture at a total ion source pressure of 0.50 Torr is shown in Figure 2a. Peaks are observed at *m*/*z* 90 Et_2S^+, *m*/*z* 124 $[Me_2S\therefore SMe_2]^+$, *m*/*z* 152 $[Et_2S\therefore SMe_2]^+$, and *m*/*z* 180 $[Et_2S\therefore SEt_2]^+$. No peak at *m*/*z* 62 corresponding to Me_2S^+ was ever observed. This implies a bimolecular charge transfer from Me_2S^+ to Et_2S and/or charge transfer upon dissociation of the adduct. The peak at *m*/*z* 124 from $[Me_2S\therefore SMe_2]^+$ was usually not very intense.

As the ionizing electron energy was raised to 12.5 eV, new peaks appeared in the mass spectrum (Figure 2b). Peaks at *m*/*z* 123, 137, 151, and 165 increase in intensity with increasing energy. We propose that the ions which appear at higher electron energies originate from reactions of fragment ions. The reactions shown below could give rise to the observed masses.

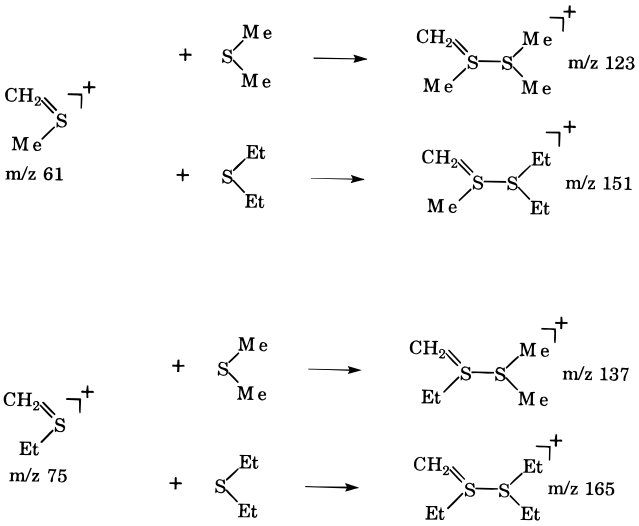

The data imply that at higher electron energies, *m*/*z* 61 and 75 are formed from the parent neutrals by fragmentation. The ions then react with the neutral molecules present in the ion source. It is not known from these spectra if any of these ions could also result from association reactions followed by long-lived fragmentation. This point will be returned to in the section on the MS/MS results.

In addition, at even higher electron energies in the range 30−70 eV, other peaks corresponding to P + 1 ions appear and become quite prominent. Though the ions appearing at higher electron energies did not appear to shift the equilibrium constants, all equilibrium measurements were made using low ionizing electrons where only *m*/*z* 90 Et_2S^+, *m*/*z* 124 $[Me_2S\therefore SMe_2]^+$, *m*/*z* 152 $[Et_2S\therefore SMe_2]^+$, and *m*/*z* 180 $[Et_2S\therefore SEt_2]^+$ were observed in the spectra.

Thermodynamic Equilibrium Measurements. The thermodynamic reaction enthalpies and entropies were determined by the dependence of the equilibrium constant on temperature as given by the van't Hoff equation:

$$\ln K_p = -\Delta H^\circ_{rxn}/RT + \Delta S^\circ_{rxn}/R \qquad (1)$$

For association reactions, $\Delta H^\circ_{bond} = -\Delta H^\circ_{rxn}$ for the bond

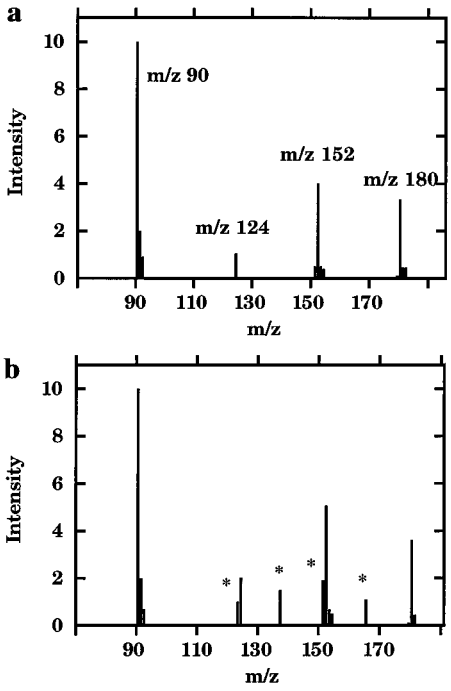

Figure 2. Reconstructed mass spectra recorded with the DuPont mass spectrometer at 491 K. The gas composition was 0.008 Torr of a 18% Et_2S in Me_2S mixture with N_2O bath gas added for a total ion source pressure of 0.40 Torr. Spectra a and b were recorded with nominal ionizing electron energies of 10 and 15 eV, respectively. The peaks appearing only at the higher electron energies are denoted by an asterisk in b.

formed in the chemical reaction, and in turn, the bond energy is related to the bond enthalpy through a heat capacity correction:

$$D^\circ_o = -\Delta H^\circ_{T,rxn} + \int_o^T \Delta C_p(T)\,dT \qquad (2)$$

where ΔC_p is the heat capacity difference between the products and the reactants. In this work statistical mechanical heat capacity corrections to the experimental bond enthalpy are made with the *ab initio* computed molecular parameters.

The equilibrium reactions observed in the Et_2S and Me_2S mixtures are:

$$Et_2S^+ + Me_2S + M \rightleftarrows [Et_2S\therefore SMe_2]^+ + M \qquad (3)$$

$$Et_2S^+ + Et_2S + M \rightleftarrows [Et_2S\therefore SEt_2]^+ + M \qquad (4)$$

Since Et_2S has a lower IP than Me_2S (8.43 eV versus 8.710 eV)[7,8] charge transfer results in Et_2S^+ rather than Me_2S^+ and both reactions 3 and 4 should approach equilibrium simultaneously. Various tests, including time-resolved experiments, are applied to determine if equilibrium has been established.[18] Residence time distributions (RTD) are measured for all ions involved in an equilibrium. If the normalized RTD's are identical, the system should be at equilibrium since the charge that is ultimately measured undergoes many switching reactions as it traverses the source. The actual RTD for the ions are then a weighted average of the drift properties. When the RTD's are identical, the ion current ratios are constant over the entire

(18) One of the criteria which is used in our experiments to convincingly demonstrate attainment of equilibrium is the superimposability of residence−time distributions for all ions involved in the equilibrium. Residence−time distributions of ions in equilibrium **must** be the same since the charge that is detected undergoes many switching reactions as it traverses the source. The switching reactions result in an averaging of the drift properties (mobility and diffusion).

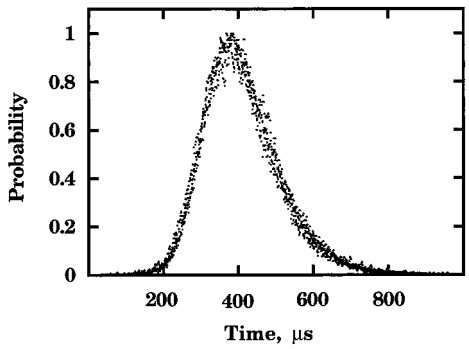

Figure 3. Residence time distributions of Et_2S^+, $[Me_2S\therefore SMe_2]^+$, $[Et_2S\therefore SMe_2]^+$, and $[Et_2S\therefore SEt_2]^+$. The superimposability of the four distributions demonstrates that all four ions are in chemical equilibrium.

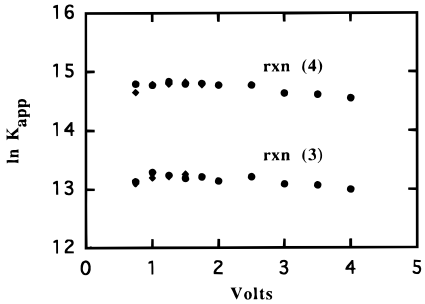

Figure 4. Plots of ln *K* verses the ion source voltage at different total ion source pressures for reactions 3 and 4. The ion source composition was 0.06 Torr of 18% Et_2S in Me_2S at total ion source pressures of 0.225 Torr (diamonds) and 0.325 Torr (filled circles).

time covered. We have found that identical RTD's are a necessary condition for establishing chemical equilibrium.

Figure 3 shows typical RTD's for Et_2S^+, $[Me_2S\therefore SMe_2]^+$, $[Et_2S\therefore SMe_2]^+$, and $[Et_2S\therefore SEt_2]^+$ and demonstrates that both reactions 3 and 4 are in chemical equilibrium since the distributions for the ions involved in the reactions are identical. Apparent equilibrium constants were also measured at various gas compositions, total ion-source pressures, and as a function of ion extraction fields (ranges are given in the Experimental Section). The equilibrium constants extrapolated to zero ion source voltages were used to construct the van't Hoff plots. Figure 4 shows typical ln K_p vs extraction voltage plots at two temperatures for reactions 3 and 4. The plots appear flat over most of the voltage range and demonstrate that the equilibrium constants are independent of the applied voltage and hence the ions are not appreciably heated by the applied field. At each temperature, the extrapolated values of the zero-field ln K_p with varying compositions and total pressures are all the same. Each of the tests above indicate that chemical equilibrium has been achieved.

The van't Hoff plots shown in Figure 5 are determined from ln K_p values extrapolated to zero extraction volts. The equilibrium constants K_p are determined by varying the Et_2S to Me_2S compositions and varying total ion-source pressures using N_2O as a bath gas. The results obtained from these data for reactions 3 and 4 are $\Delta H^\circ_{506K,rxn(3)} = -104 \pm 1.5$ kJ/mol, $\Delta S^\circ_{506K,rxn(3)} = -118 \pm 3$ J/(mol·K), $\Delta H^\circ_{506K,rxn(4)} = -119 \pm 1.5$ kJ/mol, and $\Delta S^\circ_{506K,rxn(4)} = -137 \pm 3$ J/(mol·K), where the errors are the result of a standard least-squares analysis. The reaction enthalpy for reaction 3 leading to the unsymmetric 2c−3e bonded complex is less exothermic than those previously reported for the symmetric complexes $[Me_2S\therefore SMe_2]^+$ and $[Et_2S\therefore SEt_2]^+$ as well as the present result for reaction 4 leading to $[Et_2S\therefore SEt_2]^+$. This finding agrees with the arguments presented above concerning the bonding in unsymmetric systems as influenced by orbital energy matching. The present results

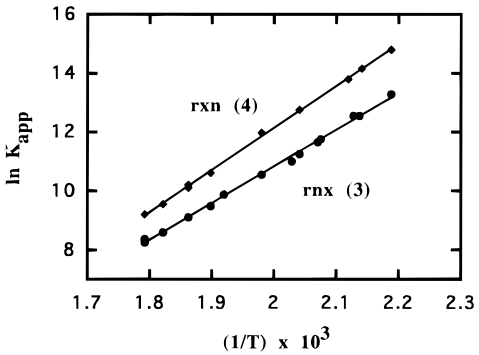

Figure 5. The van't Hoff plots resulting from the extrapolated data such as that shown in Figure 4.

for reaction 4 are in excellent agreement with our previously published value for this reaction studied with neat Et_2S in a bath gas where the experimental values for the enthalpy and entropy of reaction 520 K were found to be $\Delta H^\circ_{520K,rxn(4)} = -116$ kJ/mol and $\Delta S^\circ_{520K,rxn(4)} = -132$ J/(mol·K).

The values for the entropies of reaction are not considered to be as reliable as those previously published in other studies due to the method by which the gas mixtures were prepared and introduced into the mass spectrometer. An error in the ion-source gas composition will affect only the intercept of eq 1 and hence the entropy of reaction. This holds as long as the fraction by which the composition varies from the presumed composition is temperature independent. Under such circumstances the slopes and hence the enthalpies of reaction are not affected by any error in the presumed gas composition.

Figure 3 also shows that the RTD's for $[Me_2S\therefore SMe_2]^+$ is very similar to those for Et_2S^+, $[Et_2S\therefore SMe_2]^+$, and $[Et_2S\therefore SEt_2]^+$ which indicates that $[Me_2S\therefore SMe_2]^+$ is in equilibrium or close to equilibrium with the reactions 3 and 4. It is interesting to note that since Me_2S^+ is not observed in the mass spectrum, equilibrium of $[Me_2S\therefore SMe_2]^+$ with the other complexes might be achieved by the switching reaction:

$$[Et_2S\therefore SMe_2]^+ + Me_2S \rightleftarrows [Me_2S\therefore SMe_2]^+ + Et_2S \quad (5)$$

Although it would have been desirable to collect data on the equilibrium constant for reaction 5, the ion intensity for $[Me_2S\therefore SMe_2]^+$ was weak, making it difficult to experimentally study this reaction.

Another interesting point is that equilibrium is achieved faster via the ion−molecule switching reaction 6 than the association equilibrium 3 and 4. This conclusion is reached by considering the RTD's in Figure 6.

$$[Et_2S\therefore SMe_2]^+ + Et_2S \rightleftarrows [Et_2S\therefore SEt_2]^+ + Me_2S \quad (6)$$

At higher extraction voltages and lower total ion-source pressures, the RTD's for all three ions in eqs 3 and 4 are not identical even though the RTD's for the two association products are identical (in equilibrium). This implies that $[Et_2S\therefore SMe_2]^+$ and $[Et_2S\therefore SEt_2]^+$ are in chemical equilibrium with each other but not with Et_2S^+. The switching reaction 6 would account for these observations since it interchanges the charge in bimolecular reactions which should be faster than the association reactions. It should be recognized that the mobilities for $[Me_2S\therefore SEt_2]^+$ and $[Et_2S\therefore SEt_2]^+$ would be expected to be similar and the near-identical RTD's in Figure 6 could reflect this fact as well as the switching reaction given in eq 6.

Theoretical Results. Calculated absolute and relative energies of Me_2S, Et_2S, Et_2S^+, $[Et_2S\therefore SMe_2]^+$, and $[Et_2S\therefore SEt_2]^+$ were computed at the PMP2 and DFT level. The absolute results are presented in Table 1 while the relative results are

Table 1. Total Energies (hartrees), Zero-Point Energies (kJ/mol), Heat Capacity Corrections at 298 K (kJ/mol), and Entropies at 298 K (J/(mol·K))[a]

		//HF/6-31G(d)					//B3LYP/6-31G(d)			
	PG	HF	MP2	ZPE(NIF)[b]	C_p[c]	S	B3LYP	ZPE(NIF)[b]	C_p[c]	S
Me_2S	C_{2v}	−476.73533	−477.12111	214.1(0)	14.8	280.4	−478.01381	200.3(0)	15.3	283.8
Et_2S	C_{2v}	−554.80562	−555.45408	375.4(0)	21.3	342.8	−556.64253	353.5(0)	22.2	350.2
Et_2S	C_2	−554.80429	−555.45400	375.5(0)	20.9	342.8	−556.64224	353.5(0)	21.8	346.8
Et_2S	C_1	−554.80496	−555.45402	375.4(0)	21.2	348.0	−556.64235	351.9(0)	21.9	354.0
Me_2S^+	C_{2v}	−476.45471	−476.81777	211.6(0)	15.7	295.0	−477.69910	196.3(0)	16.4	304.3
Et_2S^+	C_{2v}	−554.53569	−555.15955	372.6(1)	22.2	360.6	−556.33929	346.9(1)	20.9	347.1
Et_2S^+	C_2	−554.53390	−555.15908	374.3(0	21.7	353.5	−556.33879	349.6(0)	22.7	360.9
Et_2S^+	C_1	−554.53475	−555.15928	373.5(0)	21.9	362.7	−556.33915	348.5(0)	22.8	369.1
Et_2S^+ [d]	C_2						−556.33938	347.2(0)	23.2	369.2
$Me_2S\therefore SMe_2^+$	C_{2h}	−953.21556	−953.98664	433.1(0)	31.0	433.0	−955.76476	404.6(0)	32.8	450.4
$Et_2S\therefore SMe_2^+$	C_1	−1031.28784	−1032.32273	594.5(0)	37.5	495.7	−1034.39692	556.4(0)	39.4	513.9
$Et_2S\therefore SEt_2^+$	C_2	−1109.36159	−1110.66046	754.6(0)	44.6	552.1	−1113.02971	705.6[e]	47.0[e]	573.1[e]

[a] Total energies and related properties for Me_2S, Me_2S^+, Et_2S^+, Et_2S^+, $Me_2\therefore SMe_2^+$, and $Et_2S\therefore SEt_2^+$ at the PMP2 level are from ref 2. [b] Zero-point energy (kJ/mol) with number of imaginary frequencies in parentheses. [c] Integrated C_v (from 0 to 298 K) + RT. [d] This C_2 structure of Et_2S^+ is only slightly distorted from the Et_2S^+ C_{2v} structure. [e] Corrections at the DFT level for $[Et_2S\therefore SEt_2]^+$ were estimated by scaling the HF/6-31G(d) value by the B3LYP/6-31G(d):HF/6-31G(d) ratio for the zero-point energy (0.935), heat capacity corrections (1.058), and entropy (1.038) computed from the $[Me_2S\therefore SMe_2]^+$ and $[Et_2S\therefore SMe_2]^+$ complexes.

Table 2. Calculated Bond Energies (kJ/mol), Bond Enthalpies at 298 K (kJ/mol), and Association Entropies 298 K (J/(mol·K)) for Forming 2c−3e S∴S Bonds

	//HF/6-31G(d)					//B3LYP/6-31G(d)			
	HF	PMP2	+ZPE	+C_p 298 K	S	B3LYP	+ZPE	+C_p 298 K	S
$Me_2S\therefore SMe_2^+$	66.9	125.5	118.8	118.4	−142.2	136.0	128.0	127.2	−137.6
$Et_2S\therefore SMe_2^+$ [a]	46.4	110.9	104.6	103.7	−147.3	114.6	105.8	105.0	−138.9
$Et_2S\therefore SEt_2$ [b]	57.3	123.8	118.8	117.1	−158.6	125.5	118.8[c]	117.1[c]	−146.4[c]

[a] The reference monomer cation (Et_2S^+) has C_{2v} symmetry at the PMP2 level and C_2 symmetry at the DFT level. [b] At the PMP2 level, Et_2S and Et_2S^+ have C_{2v} symmetry. At the DFT level, the Et_2S reference has C_{2v} symmetry, while the Et_2S^+ reference has C_2 symmetry. [c] Zero-point and heat capacity corrections and entropies at the DFT level for $[Et_2S\therefore SEt_2]^+$ were estimated by scaling the HF/6-31G(d) value. See Table 1 footnote *d*.

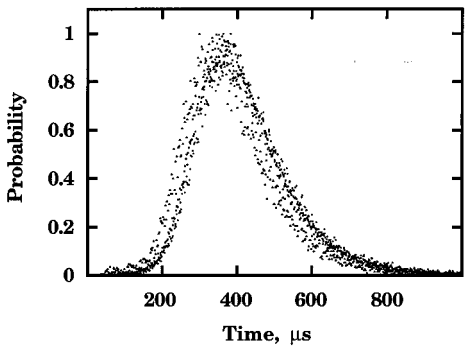

Figure 6. Residence time distributions of Et_2S^+, $[Et_2S\therefore SMe_2]^+$, and $[Et_2S\therefore SEt_2]^+$ under conditions where $[Et_2S\therefore SMe_2]^+$ and $[Et_2S\therefore SEt_2]^+$ have reached equilibrium with each other but not with Et_2S^+. The "leading" distribution is that for Et_2S^+. We propose that the equilibrium between $[Et_2S\therefore SMe_2]^+$ and $[Et_2S\therefore SEt_2]^+$ is achieved by the switching reaction 6.

presented in Table 2. In the present study, our previous calculations of the Et_2S and Et_2S^+ conformers at the PMP2 level[2] have been extended to the DFT level. For neutral Et_2S at the DFT level, three conformers are very close in energy (Table 1). The more symmetrical C_{2v} structure was chosen as the reference monomer for neutral Et_2S since the three conformers are within about 0.4 kJ/mol at both the PMP2 and DFT levels. For the Et_2S^+ radical cation, the situation is a bit more complex. At the PMP2 level, the C_{2v} structure is more stable, while at the B3LYP/6-31G(d) the C_{2v} structure has one imaginary frequency. A slight distortion to C_2 symmetry lowers the B3LYP/6-31G(d) energy by less than 0.4 kJ/mol. Zero-point and heat capacity corrections reverse the relative stability of the C_{2v} and C_2 structures. However, if the C_{2v} structure was indeed the true minimum, the imaginary frequency should be real and therefore contribute to the zero-point and heat capacity corrections. While the C_{2v} conformer of Et_2S^+ was chosen as the reference in the previous work at the PMP2 level, here we choose the slightly distorted C_{2v} (C_2 symmetry) structure as the Et_2S^+ reference at the DFT level. With this choice, all reference structures are lowest in energy at 0 K and are minima on the respective electronic potential energy surface.

Figure 7a shows the lowest energy DFT structures for Et_2S^+, Me_2S, and $[Et_2S\therefore SMe_2]^+$ while Figure 7b shows those for Et_2S^+, Et_2S, and $[Et_2S\therefore SEt_2]^+$. As pointed out in our previous study of $[Et_2S\therefore SEt_2]^+$,[2] the C_1 conformers of Et_2S and Et_2S^+ are more appropriate for forming an ion−molecule complex because there is a better compromise between intra- and intermoiety repulsion. In forming the ion−molecule complex $[Et_2S\therefore SMe_2]^+$ between Et_2S^+ and Me_2S at the DFT level, the Et_2S^+ moiety adopts a slight distortion of the C_2 symmetry conformer.[19] While slightly higher in energy than the other conformers (Table 1), the C_2 conformer is able to associate with Me_2S with little intermoiety repulsion.

At the DFT level the calculated S∴S 2c−3e bond energy in $[Et_2S\therefore SMe_2]^+$ is 107.8 kJ/mol which is in excellent agreement with the experimental bond energy of 107 kJ/mol obtained by applying the heat capacity correction determined from the *ab initio* data. At the same level, the computed 2c−3e sulfur−sulfur bond length is 2.965 Å which can be compared to an average sulfur−sulfur 2c−2e bond length of 2.05 Å.[20] The calculated value for $\Delta S°_{506,rxn}$ for reaction 3 (−139 J/(mol·K)) at the DFT level is somewhat more negative than the experimental value (−118 kJ/(mol·K)). However, as indicated above, the experimental values for the entropies of reaction must be viewed with caution. DFT predicts the unpaired electron in a σ^*_{ss} orbital localized between the two sulfur atoms with the

(19) Note: This is not the $C_{2v} \rightarrow C_2$ structure discussed in the text which is only a slightly distorted C_{2v} structure.

(20) (a) Knop, O.; Boyd, R. J.; Choi, S. C. *J. Am. Chem. Soc.* **1988**, *110*, 7299. (b) Allen, F. H.; Kennard, O.; Watson, D. G.; Brammer, L.; Orpen, A. G.; Taylor, R. *J. Chem. Soc., Perkin Trans. 2* **1987**, S1.

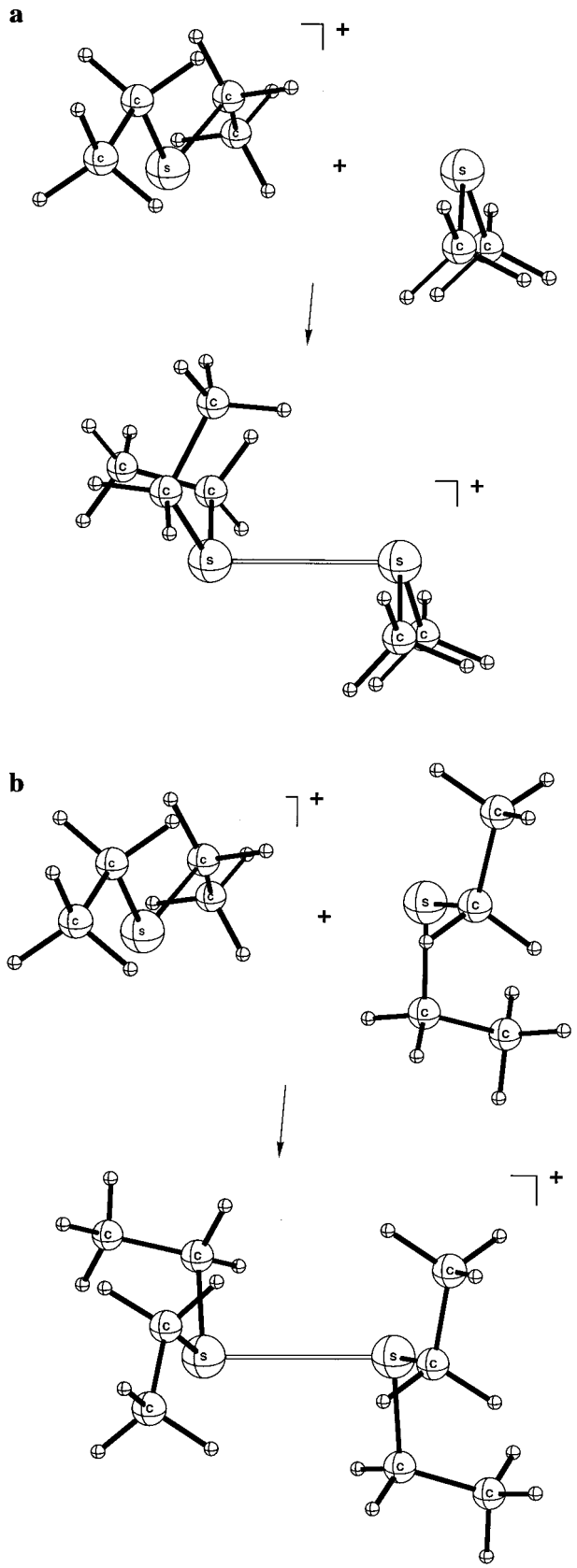

Figure 7. Calculated structures at the B3LYP/6-31G(d) level (a) for the species in reaction 3 and (b) for those in reaction 4.

unpaired α spin density to be nearly evenly distributed between the Et_2S sulfur (0.51) and Me_2S sulfur (0.47). This suggests that in the gas phase there is little charge-spin separation due to the different substituent on the sulfurs. We are investigating whether the charge-spin separation for this system increases in solution.

Table 3. Calculated[a] and Experimental Adiabatic Ionization Potentials (eV)

		PMP2	DFT	Δ(DFT−PMP2)	exptl	Δ(exptl−DFT)
Me_2S	$(C_{2v} \rightarrow C_{2v})$	8.25	8.56	0.31	8.71[b,c]	0.15
Et_2S	$(C_{2v} \rightarrow C_{2v}/C_2)$[d]	8.01	8.25	0.24	8.43[b]	0.18

[a] "PMP2" level is PMP2/6-31G(d)//HF/6-31G(d); "DFT" level is B3LYP/6-31G(d)//B3LYP/6-31G(d). Zero-point and heat capacity corrections are not included. [b] Reference 7. [c] Reference 8. [d] The reference cation (Et_2S^+) has C_{2v} symmetry at the PMP2 level and C_2 symmetry at the DFT level.

Clark[21] has proposed eq 7 for estimating the binding energies of unsymmetric odd-electron bonds.

$$D_{AB} = {}^1/_2(D_{AA} + D_{BB})\exp(-\lambda_A\lambda_B\Delta IP) \qquad (7)$$

D_{AB}, D_{AA}, and D_{BB} are the binding energies of the unsymmetric and symmetric complexes, ΔIP is the difference in ionization potentials for the two neutral molecules (in kJ/mol), and λ_A and λ_B are adjustable parameters. If one assumes that λ_A and λ_B are the same and uses the DFT values of 105.8, 128.0, and 118.8 kJ/mol for D_{EtMe}, D_{MeMe}, and D_{EtEt} respectively, then $\lambda_{Me} = \lambda_{Et} = 0.649$ (mol/kJ)$^{1/2}$. Clark reports a somewhat smaller λ value for H_2S $\{\lambda = (0.544$ mol/kJ$)^{1/2}\}$. No physical meaning has been correlated with λ and further interpretation is not possible.

The calculated results for $[Et_2S\therefore SEt_2]^+$ at the DFT level compared very well with the previously published calculations at the MP2 level except for the sulfur−sulfur bond length which is longer (2.968 Å) at the DFT level compared to the MP2 level (2.870 Å). However, the bond energies at the DFT and PMP2 levels are similar, 118.8 and 117.0 kJ/mol, respectively. Utilizing the calculated parameters to scale the present experimental values results in a reaction enthalpy at 298 K of −122 kJ/mol and a bond energy of 123 kJ/mol.

Table 3 presents the calculated and experimental ionization energies for Et_2S and Me_2S, at the PMP2 and DFT levels. Although too low by about 0.15 eV, the DFT values are uniformly in better agreement with experiment than are the PMP2 values.

MS/MS Collision-Induced Dissociation and Metastable Experiments. In previous studies on 2c−3e bonds the structures of the species involved have been assigned from chemical intuition and *ab initio* results but there has been little or no experimental confirmation on the structures or atomic connectivity. In order to gain additional experimental evidence for the structure of $[Et_2S\therefore SMe_2]^+$, MS/MS experiments on our modified ZAB-1F were carried out. CID experiments provide more direct evidence for molecular structures than do metastable experiments since the fragmenting ions are shorter lived and in general have not undergone structural isomerization. The CID spectrum of $[Et_2S\therefore SMe_2]^+$ is shown in Figure 8. The most intense peak is *m*/*z* 90 corresponding to Et_2S^+. Since one expects the 2c−3e bond to be the weakest bond in the molecule and since Et_2S has a lower ionization potential than Me_2S,[7,8] this result strongly supports the 2c−3e bonded structure. Weaker peaks at *m*/*z* 47, 62, 75, 108, 123, and 137 are assigned in Figure 8. These fragments are consistent with the proposed molecular connectivity. All but one of these peaks (that at *m*/*z* 75) could originate by direct cleavage of skeleton atoms in $[Et_2S\therefore SMe_2]^+$. The peak at *m*/*z* 75 has the same mass as that proposed for the reactant ion giving rise to *m*/*z* 137 and 165 in the high-energy, high-pressure mass spectra. The results suggest that the $[RS{=}CH_2]^+$ group (where R is either Me or Et) can originate both by direct fragmentation and by fragmentation from the association complex. However, a rearrangement (to

(21) Clark, T. *J. Am. Chem. Soc.* **1988**, *110*, 1672.

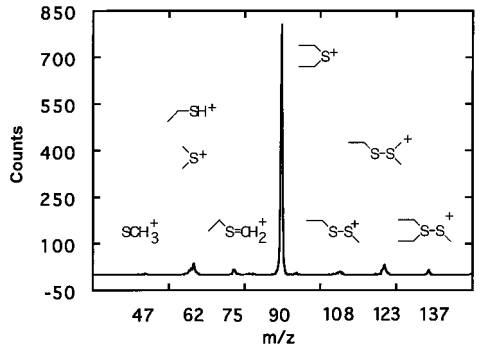

Figure 8. Collision-induced dissociation spectrum of *m*/*z* 152.

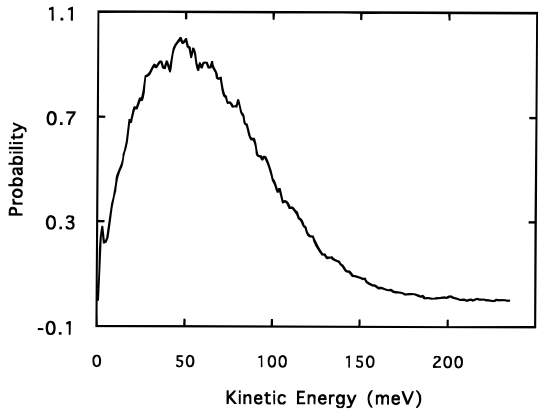

Figure 9. Metastable kinetic energy release distribution for $[Et_2S\therefore SMe_2]^+ \rightarrow Et_2S^+ + Me_2S$.

the structure shown below) within the association complex prior to fragmentation cannot be excluded.

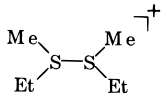

Metastable peaks can originate from long-lived energized parent structures or from long-lived energized species which sample other isomers, hence metastable spectra often are not as diagnostic of atomic connectivity as are CID spectra.[22] In the present situation, *m*/*z* 90, which has been assigned as Et_2S^+, is the only metastable ion observed in the metastable spectrum of $[Et_2S\therefore SMe_2]^+$. Clearly this result is consistent with the IP's of the two moieties and supports the CID data. The kinetic energy release distribution (KERD) obtained from the metastable peaks shape by standard methods[23] is shown in Figure 9. The distribution shape and the average kinetic energy release (0.028 eV) support a statistical unimolecular fragmentation process.[24] The shape of the KERD is also characteristic of a reaction with no reverse activation barrier.

The High-Pressure Mass Spectrum of $[H_2S\therefore SMe_2]^+$. A natural extension of this work would be the investigation of $[H_2S\therefore SMe_2]^+$. Since the ionization potential difference for H_2S and Me_2S ($\Delta IP = 2.742$ eV)[7] is larger than that for Et_2S and Me_2S ($\Delta IP = 0.28$ eV),[7,8] a weak 2c−3e bond is expected. However, the mass spectra of mixtures of H_2S and Me_2S in N_2O at 300 K do not have a peak at *m*/*z* 96 which could correspond to $[H_2S\therefore SMe_2]^+$. Instead the peaks observed at low ionizing electron energies were *m*/*z* 62 Me_2S^+ and *m*/*z* 124 $[Me_2S\therefore SMe_2]^+$. The absence of a 2c−3e bonded species corresponding to $[H_2S\therefore SMe_2]^+$ indicates that this molecule is too weakly bound to be observed at the lowest feasible experimental temperature, 298 K (experiments at lower temperatures were not possible due to condensation of the sample).

Conclusions

The data presented support the 2c−3e interpretation for the bond in the unsymmetric radical cation $[Et_2S\therefore SMe_2]^+$ and represent the first experimental evidence for the atomic connectivity in the adducts formed in the high-pressure ion sources. Experimentally, chemical equilibrium for reaction 3 was established from to 467 to 559 K resulting in a reaction enthalpy of −104 kJ/mol from the van't Hoff equation. Applying heat capacity corrections to 0 K results in a corrected experimental bond energy of 107 kJ/mol, which is in excellent agreement with the *ab initio* value (107.8 kJ/mol) at the B3LYP/6-31G(d)+ZPC level of theory. The computed spin density is 0.51 on the Et_2S sulfur and 0.47 on the Me_2S sulfur. Residence time distributions for all the ions suggest that the charge transfer switching reaction 6 is faster than the charge transfer resulting from association steps.

MS/MS CID and metastable experiments are strongly supportive of the proposed atomic connectivity and hence the 2c−3e nature for the sulfur−sulfur bond. The average metastable kinetic energy release, 0.028 eV, and the kinetic energy release distribution (KERD) shape for the reaction $[Et_2S\therefore SMe_2]^+ \rightarrow Et_2S^+ + Me_2S$ is indicative of a statistical unimolecular process with a small or no reverse activation barrier.

The symmetric $[Et_2S\therefore SEt_2]^+$ complex was observed through a competing process reaction 4. The experimental reaction enthalpy at 506 K was found to be −119 kJ/mol. Corrected to 0 K this results in a bond energy of 123 kJ/mol which can be compared to a computed bond energy at the DFT level (B3LYP/6-31G(d)+ZPC) of 118.8 kJ/mol. These findings are in very good agreement with our previously published experimental and computational values.[2]

Acknowledgment. A.J.I. is very grateful to the donors of the Petroleum Research Fund administered by the American Chemical Society and to BASF-Germany for the donation of the ZAB-1F without which the MS/MS studies would not have been possible. M.A.J. acknowledges the DOE for a Patricia Roberts Harris graduate fellowship. A generous allocation of computer time was provided by the Alabama Supercomputer Network and the NFS-supported Pittsburgh Supercomputer Center. The Auburn University Chemistry Department provided valuable financial and technical support. Finally, we thank Dr. Michael Peschke for many helpful discussions.

JA960455H

(22) (a) Jennings, K. R. *Int. J. Mass Spectrom. Ion Phys.* **1968**, *1*, 227. (b) McLafferty, F. W.; Kornfeld, R.; Haddon, W. F.; Levsen, K.; Saka, I.; Bente, P. F., III; Tsai, S.-C.; Schuddemage, H. D. R. *J. Am. Chem. Soc.* **1973**, *95*, 3886. (c) McLafferty, F. W.; Bente, P. F., III; Kornfeld, R.; Tsai, S.-C.; Howe, I. *J. Am. Chem. Soc.* **1973**, *95*, 2120.

(23) Jarrold, M. F.; Illies, A. J.; Kirchner, N. J.; Wagner-Redeker, W.; Bowers, M. T.; Mandich, M. L.; Beachamp, J. L. *J. Phys. Chem.* **1983**, *87*, 2213.

(24) Jarrold, M. F.; Wagner-Redeker, W.; Illies, A. J.; Kirchner, N. J.; Bowers, M. T. *Int. J. Mass Spectrom. Ion. Process.* **1984**, *58*, 63.